ACS Sustainable Chemistry & Engineering

Research Article

pubs.acs.org/journal/ascecg

Mathematical Modeling of Fast Biomass Pyrolysis and Bio-Oil Formation. Note I: Kinetic Mechanism of Biomass Pyrolysis

Eliseo Ranzi,* Paulo Eduardo Amaral Debiagi, and Alessio Frassoldati

Dipartimento di Chimica, Materiali e Ingegneria Chimica "Giulio Natta", Politecnico di Milano, Piazza Leonardo da Vinci, 32, 20133 Milano, Italy

Supporting Information

ABSTRACT: This paper discusses the research activities done at Politecnico di Milano in the field of the detailed kinetic modeling of pyrolysis and combustion of biomass and bio-oil formation. Different critical steps are involved in this multicomponent, multiphase and multiscale problem. The first complexity relies on biomass characterization with the selection of reference species: cellulose, hemicellulose, lignins, and extractives. Fast pyrolysis involves kinetic mechanisms, first in the solid phase for biomass pyrolysis, then in gas-phase for secondary reactions of released products. These mechanisms involve large number of species and reactions, which make computations expensive. They need to be simplified, while still maintaining their description capability. Lumping procedures are extensively applied to allow the development of the overall model. Multistep pyrolysis mechanisms of reference species are discussed in this Note, with several comparisons with experimental data. A peculiarity of the model is its ability to provide detailed compositions of pyrolysis products and solid residue. Catalytic effect of ash on pyrolysis products is also discussed. A companion paper will discuss the successive or secondary gas phase reactions of pyrolysis products, together with the heterogeneous reactions of residual char. Finally, the modeling of bio-oil formation requires a comprehensive description of the coupling of kinetic and transport processes, both at the particle and the reactor scale.

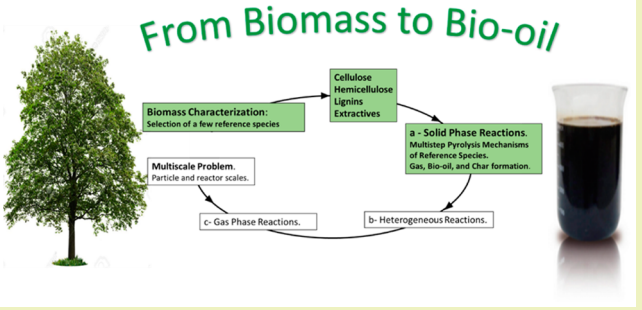

KEYWORDS: *Fast biomass byrolysis, Biomass characterization, Cellulose, hemicellulose, lignin, and extractives, Multistep kinetic mechanism of biomass decomposition, Ash effect on pyrolysis products*

INTRODUCTION

Lignocellulosic biomass is a promising option for reducing global dependence on fossil fuels, and it can give valuable materials through different routes including thermal, biological, and physical processes. Thermal biomass conversion gives multiple and complex products, often in short reaction times, with or without inorganic catalysts used to improve the product quality. Pyrolysis is the thermal treatment of biomass in the absence of oxygen producing liquid fuels, together with some residual char and a fuel gas.[1] Coal pyrolysis has been applied for several years, but only recently has fast biomass pyrolysis for producing bio-oil reached an industrial interest.[2] At temperatures of ∼750−800 K and very short reaction times, this process gives yields up to 75−80 wt % of liquid fuels. High temperature pyrolysis produces syngas, mainly constituted by H_2 and CO, which can be used either directly as fuel, or as raw material for methanol synthesis and liquid fuels.[3] Gasification is the partial oxidation of solid fuels with steam and/or air and has the possibility of combining temperature and equivalence ratio to obtain an appropriate syngas.[4] BTL (biomass-to-liquids), CTL (coal-to-liquids), and IGCC (integrated gasification combined cycle) are emerging technologies based on solid fuel gasification.[5] Biomass combustion is a well-known technology with extensive use mainly in developing countries and it requires a careful attention to environmental problems. Along with these thermochemical utilizations of biomass, other biological processes typically produces ethanol, via fermentation, or biogas through anaerobic digestion.

The main subject of this paper is to analyze the kinetics of biomass pyrolysis, which is the first step toward bio-oil production. The chemistry affects the evolution of a biomass particle entering the hot region of a thermal reactor at least at three different levels. First, there is the biomass pyrolysis, then the heterogeneous reactions of residual char, and finally the gas-phase reactions of volatile products. Pyrolysis is the common initial step also in the gasification and combustion process. It accounts for the primary release of gas, condensable species (tars or bio-oil), and residual biochar. The nature and relative amount of these pyrolysis products significantly vary as a function of biomass nature and process conditions.

Received: December 19, 2016
Revised: February 20, 2017
Published: February 22, 2017

DOI: 10.1021/acssuschemeng.6b03096
ACS Sustainable Chem. Eng. 2017, 5, 2867−2881

The mathematical modeling of the thermal degradation of biomass is a challenging problem because its complexity occurs at several levels:[6,7]

- Multicomponent problem. Biomass is a complex feed and it requires a proper characterization.
- Multiphase problem. Biomass reacts in a condensed phase forming a solid, a liquid, and a gas phase. Successive heterogeneous gas−solid reactions involve the biochar, whereas gas and bio-oil react in the gas-phase.
- Multiscale problem. The coupling of kinetic and transport processes needs to be considered both at particle and reactor scale.

The multiscale nature of pyrolysis process is evident when considering the angstroms of the molecular scale and the meters of pyrolysis reactors. Time-scales also vary from the very short life times of propagating radicals involved in the reacting system up to several minutes required to heat and devolatilize thick biomass particles.[7]

Note I and Note II of this work summarize and critically discuss the multistep kinetic mechanism of biomass pyrolysis initially presented by Ranzi et al.[8] More recent model extensions[9] and further improvements are also discussed. One of the peculiarities of this kinetic model, when compared to different biomass pyrolysis models, lies in its attempt and ability to provide detailed information on the compositions of gas and tar released as well as of solid residue. The overall kinetic model also includes the successive heterogeneous reactions of biochar, as well as the secondary gas phase reactions of gas and tar species released during biomass pyrolysis. These successive reactions of gas and condensed species,[10] will be discussed in Note II of this work.[11]

After this general introduction, this paper is structured as follows. The Biomass Composition section shortly describes the biomass structure and composition, together with the most important analytical methods. The biomass samples are first characterized by means of a limited number of reference components in the Biomass Characterization: Reference Species and van Krevelen Diagram section. Then, the Multistep Kinetic Mechanism of Biomass Reference Species section describes the pyrolysis behavior of these reference components with a multistep kinetic scheme. Biomass pyrolysis products are simply obtained by a linear combination of char, tar and gas products released by the individual reference components. The BIOMASS Pyrolysis and Released Products section analyzes the biomass pyrolysis model and discusses the catalytic effect of ash on pyrolysis products. Finally, some conclusions are drawn in the last section (Conclusion).

BIOMASS COMPOSITION

The capability to define the chemical composition of complex biomass materials is a first key and necessary feature for the modeling of thermochemical processes of biomass conversion to fuels and valuable chemicals. An extensive database of more than 600 biomass samples, in terms of proximate, elemental and structural analysis, is already reported elsewhere.[9] This database refers to a large number of biomass materials like wood, bark, pits, seeds, shells, energy crops, grasses, stalks, hull-husk, fibrous material, etc.

In comparison with coal, biomass has a lower density and a lower heating value. Therefore, the higher heating value of bio-oils typically ranges between 15 and 20 MJ/kg, which is only 40−50% of the one of conventional petroleum fuels (42−45 MJ/kg). This is because of the oxygen content, which is usually 35−40 on dry basis weight. Cellulose (30−55 wt %), hemicellulose (13−35 wt %), and lignin (14−36 wt %) are the major building blocks of woody biomass, whereas extractives are usually lower than 15−20%. This structural analysis is only available in less than 20% of the overall set of biomass samples.[9]

Biomass Analytical Methods. Proximate, ultimate, and structural or biochemical analyses provide information on biomass composition. Biomass samples are heterogeneous and demand reliable preparation methods. Drying, milling, acid and basic treatments with or without organic solvents, followed by chromatographic analysis, are applied in order to determine the content of cellulose, hemicellulose, and lignin. Institutions such as the National Renewable Energy Laboratory (NREL)[12] and the American Society for Testing and Materials (ASTM) are seeking to standardize preparation procedures and complete analytical methodologies.[13]

Proximate analysis is carried out with thermogravimetric analysis (TGA) in accordance with the ASTM procedure[14] and includes the determination of moisture, volatile matter, fixed carbon, and ash.

Ultimate or elemental analysis commonly decomposes the sample high-temperature oxidation. It consists in fully oxidizing the sample, and determine the composition of main atoms (C, H, N, and S) through measurement of the corresponding oxidized gases. Usually, oxygen is calculated by difference. For on line applications and environmental analyses, the fast and sensitive mass spectrometry allows to determine the elemental composition from electron ionization.[15]

Volatile matters in biomass typically span between 60 and 80%, with a fixed carbon in the range 10−20%. C, H, and O sum up to more than 95%, whereas only a few percent of N and minor amounts of S and Cl complete the elemental analysis. The amount of ash significantly varies among the different biomass samples.

The more complex structural or biochemical analysis measures the main components cellulose, hemicellulose, lignin, and sometimes also extractives and proteins. Figure 1 shows the relative concentration of several carbohydrates, lignin, extractives, and ash in different biomass samples.[16]

Proximate and ultimate analysis information are not sufficient to describe the devolatilization process. A reliable structural

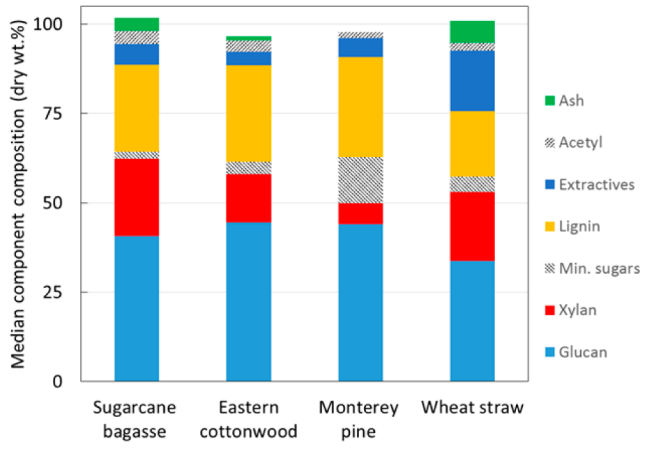

Figure 1. Typical biochemical compositions of four biomass samples[16]

DOI: 10.1021/acssuschemeng.6b03096
ACS Sustainable Chem. Eng. 2017, 5, 2867−2881

analysis of biomass samples, giving significant information on the relative content of carbohydrates (glucose, xylose, galactose, arabinose, and mannose), lignin, extractives, protein, and ash, is a valuable element if the interest is to analyze the successive biomass decomposition. Unfortunately, thermal and extraction methods can also induce some degree of decomposition.[17] Current wet chemical methods for biomass analysis are not only time-consuming and labor-intensive but also unable to provide accurate structural information. Raman and Fourier transform infrared spectroscopy provide fast and very promising results with minimal sample processing.[13,18,19]

Despite all these research efforts, detailed biochemical analyses are not commonly available, and experimental data reporting both elemental and biochemical composition remain quite scarce. This lack of information creates some difficulties in the biomasses characterization for modeling purposes, because different components undergo various decomposition pathways.

Biomass Molecular Structure. Wood and lignocellulosic biomasses are renewable and complex products usually sorted as gymnosperms and angiosperms. Gymnosperms or softwoods are evergreen, seed-producing, nonflowering plants, whose seeds are unenclosed on cones or leaves, whereas angiosperms are seasonal, seed-producing, flowering plants, whose seeds are enclosed within the fruits. Among the gymnosperms, only the conifers are major competitors with the dominant angiosperm trees. Angiosperms also include cereals and grasses.

Lignocellulosic biomass materials are mainly constituted by a combination of polysaccharides, which can be generally grouped into holocellulose (cellulose and hemicellulose) and lignin species. Moisture, together with other components such as acetyl groups, extractives, and minerals are also present.[20,21] Biomass has a porous structure where cellulose microfibril represents the important element surrounded by hemicellulose and pectin, which act as ligand and embed lignin materials.[22]

Sugars and Carbohydrates. Sugars and carbohydrates are polyhydroxylated aldehydes or ketones. Cyclic sugars with a six membered ring are called pyranoses (e.g., glucose), whereas cyclic sugars containing a five membered ring are called furanoses (e.g., fructose). There are two different isomers of glucose. In fact, the hemiacetal carbon (anomeric center) in the ring can present two configurations (anomers) with hydroxyl group in the axial plane (β) or orthogonal to the ring (α). Figure 2 shows the α and β anomers of glucose, together with the α-1,4 and β-1,4 glycosidic bond to form maltose and cellobiose, respectively. In maltose, two glucose molecules are linked by a α-1,4-glycosidic bond between the α-anomeric form

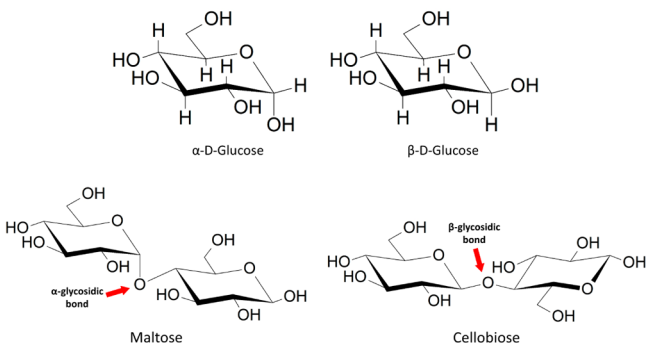

Figure 2. α and β anomers of glucose; glycosidic bonds in maltose and cellobiose.

of C-1 on one sugar and the hydroxyl oxygen atom on the C-4 of the adjacent sugar. Various glycosidic bonds are possible, because glucose has multiple hydroxyl groups. Cellobiose consists of two β-glucose molecules linked by a β-1,4 glycosidic bond, and is found as a repeat unit in cellulose. Maltose is found as a repeat unit in amylose, the linear polysaccharide in starch.

Cellulose. Cellulose, the most abundant structural polysaccharide in cell walls, comprises 15−50% of the dry weight of plant biomass. It is a linear polysaccharide composed of β-D-glucopyranose units linked by β-1,4 glycosidic bonds, which can be summarized as $(C_6H_{10}O_5)_x$, so that mass elemental composition is C = 44.4%, H = 6.2%, and O = 49.4%. Cellulose chains have a degree of polymerization (DP) of approximately 10−15 thousand of glucopyranose units in chair conformation.[23] DP of cellulose is a structural property that has a high impact on enzymatic hydrolysis, solubility, and mechanical properties of lignocellulosic biomass. The presence of several strong hydrogen bonds explains the recalcitrance of cellulose toward hydrolysis and enzyme activity. Intersheet H-bonds connect atoms between different sheets. The inchain and interchain H-bonds connect chains and thus stabilize the overall structure of cellulose fibrils, as clearly shown in Figure S1 of Supporting Information. Cellulose crystallization is directly related to the formation of these intermolecular hydrogen bonds[24]

Hemicelluloses and pectins are closely associated with the surface of cellulose fibrils with noncovalent linkages forming a microfibril network. Cell walls are further reinforced by lignin, a three-dimensional polymer of phenyl propanoid units, which is covalently linked to hemicellulose. Variations in the crystalline structure affect pyrolysis products, for example levoglucosan yield is more abundant for higher crystallinity samples.[25,26]

Hemicellulose. Hemicellulose accounts for 25−30 wt % of total biomass and is a heterogeneous complex polysaccharide derived from hexose and pentose monosaccharide units such as xylose, galactose, mannose, glucose, and arabinose. Linear or branched hemicellulose polymers are named according to the main sugar units. Mostly, sugars on hemicellulose structure are linked together by β-1,4 glycosidic bonds. Ebringerová[27] highlights three major classes of hemicellulose structures:

(a) Xylans. Linear homoxylan polysaccharides are characterized by β-1,3 and β-1,4 linkages, whereas glucuronoxylans present single side chains of α-D-glucuronic acid. L-Arabino side chains are also present in cellular wall of cereal grains.

(b) Mannans. Galactomannan, glucomannan, and galactoglucomannan polysaccharides depend on the various branching at position 6. Glucomannan is the main component in softwoods, and less abundant in hardwoods and grasses.

(c) Xyloglucans. D-Xylo-D-glucan represents the major building material of primary cell walls of all higher plants. Mixed-linkage β-glucans are present in cereals.

Galacto-glucomannan (mannose/glucose/galactose residues in a ratio 3:1:1) and glucomannan (mannose/glucose residues in a ratio of 3:1) are the prevailing components in softwood. Mannose units are acetylated at the C2 or C3 positions with one substitution every three to four units. Figure S2 exemplifies a typical structure of glucomannan polymers.

DOI: 10.1021/acssuschemeng.6b03096
ACS Sustainable Chem. Eng. 2017, 5, 2867−2881

Xylans with variable amounts of galactose, arabinose, rhamnose, methylglucuronic acid units, and acetyl groups prevail in hardwood.

The polymerization degree of hemicelluloses is relatively small (DP = 70−200), with larger molecules in hardwoods and smaller in softwoods. Very recently, Zhou et al.[28] presented detailed information on monomeric composition of hemicellulose. In most grasses and hardwoods, the xylose polymer is the primary hemicellulose constituents, and xylan conversion is important for utilization of biomass feedstocks such as corn stover, Miscanthus, switchgrass, and poplar.[29] Because of the strain in furanose units, their decomposition is faster compared with pyranose, thus indicating a greater recalcitrance of xylose with respect to arabinose. Together with hemicellulose, pectin is a major component of primary cell walls of biomass and contains highly branched polysaccharides (DP = ∼100−1000) rich in galacturonic acid.[24]

Lignin. Lignins are aromatic polymers resulting from the oxidative coupling of 4-hydroxy-phenyl-propanoid units. They contribute to make rigid and impervious the walls of secondarily thickened cells. Although lignins shield cell wall polysaccharides from microbial degradation, this protection is a limiting factor in the conversion to pulp or biofuels. Lignins are complex racemic polymers derived from three hydroxycinnamyl alcohol monomers that differ in their methoxylation degree: *p*-coumaryl, coniferyl, and sinapyl alcohols. These monolignols produce *p*-hydroxyphenyl (H), guaiacyl (G), and syringyl (S) propanoid units, and these are the main building blocks of lignin.[30,31] Figure 3 schematically shows the monolignols and the corresponding phenylpropanoid units.

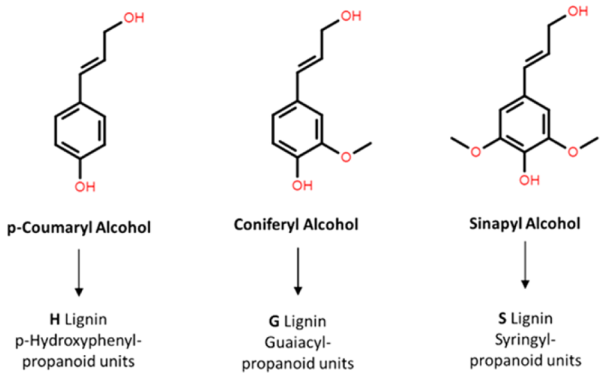

Figure 3. Monolignols and derived phenyl-propanoid units.

Hardwood lignins are mainly constituted of guaiacyl (G) and syringyl (S) units with only traces of *p*-hydroxyphenyl (H) units. Softwood lignins are mostly composed by guaiacyl (G) units with low amounts of *p*-hydroxyphenyl. Lignins in forages are composed primarily of H, G, and S units. H-units are elevated in softwood compression wood and are slightly higher in grasses.[31,32]

Several characteristic interunit linkages of lignin structure are shown in Figure S3 of the Supporting Information, where a brief discussion is also included. Lignins are generally more branched in gymnosperms than in angiosperms, because of the lack of S units. The G/S-rich lignin of angiosperms is rich in *β*-O-aryl ether linkages and cross-linked to cell wall polysaccharides.[17]

Extractives. Extractives species grasp all nonstructural substances produced by plants and are sorted as hydrophobic resins and phenolic hydrophilic species. Typical content of extractives in lignocellulosic biomass varies from 5 to 15 wt %. Bark and residues from oily seed processing are particularly rich in extractives.

Resins. Hydrophobic resins are soluble into alcohols, ethers, and chloroform. Softwood plants are usually rich in oil resins, reaching up to 15 wt % for *Pinus siberica*. Resins are composed by 60−70% of terpenes, together with fatty acids. Terpenes are hydrocarbons derived from isoprene monomers, with or without substituted groups. Limonene and pinene are monoterpenes, whereas abietic and pimaric acids are diterpenes, and several poly terpenes are also present. Low and high-molecular weight fractions are present in softwood oil-resin. The low molecular weight fraction constitutes ∼30% of the total oil-resin (turpentine). The remaining heavier terpenes together with fatty acids are the colophony.

Hardwoods usually present less than 1 wt % of wood-resin, with minor amount of terpenes. It is composed mainly by fatty acids (60−90%), mostly esterified into triglycerides. Linoleic acid ($C_{18}H_{32}O_2$) is the most abundant fatty acid both in wood and vegetable oils. Figure 4 shows typical molecules and structures of mono-, di-, and tetra-terpenes.

Phenolic Compounds. Phenolic species are usually more present in evergreen plants than in annual crops. The bark contains high amount of phenolic species, which provide extra protection to the plant.[33]

Phenolics are sorted as flavonoids and nonflavonoids. Flavonoids are molecules composed by two aromatic rings connected by three carbon and one oxygen atoms, and are usually bond to sugars. Figure 4 shows the typical flavonoid structure of cathechin. Phenolic acids and tannins constitute the nonflavonoid extractives. Tannins are made up by polymerization of flavonoids (condensed tannins) and by phenolic acids esterified with sugars (Hydrolyzable Tannins). As shown in Figure 4, the prevailing condensed tannins are connected by 4−8 (regular) or 4−6 (branching) intermonomeric bonds. Phenolic acids together with coniferyl alcohol, sinapic, and coumaric acids are the precursors of lignin building blocks.[34]

Nitrogen, Sulfur, Ash, and Inorganics. Together with C/H/O, elemental analysis gives nitrogen and sulfur content by measuring NO_x and SO_x. Both N and S components are present in greater amounts in fast-growing and young tissues such as leaves and stems. Together with minor amounts of nucleic acids, chlorophyll, amino sugars, and alkaloids, most of nitrogen and around 60% of sulfur is present as amino acids.[35] The residual sulfur content, in the form of sulfates, remains partially in ash. Ash is formed by combusting inorganics under controlled conditions. The ashing temperature for biomass is 550 °C, whereas is 780 °C for coals. Chlorine, potassium, and sodium are readily released during high temperature combustion. The wood ash content is typically less than 1 wt %, whereas in grass it ranges from 2% to 10% or even up to 25% in rice husks. The ash content is sorted as major and minor elements. Major elements include Al, Ca, Fe, Mg, P, K, Si, Na, and Ti and are expressed in terms of their oxides. They have a major impact on ash melting, fouling and corrosion, whereas they have a low impact on environment. Herbaceous biomass are rich in K and Na have higher Si, and lower Ca content compared to wood. Typically, Ca and Mg increase the ash melting temperature, whereas Si, K, and Na decrease it. Thus, grass ashes have low melting temperatures, whereas higher melting temperatures are expected for wood samples. Minor elements include As, Cd, Co, Cr, Cu, Hg, Mn, Mo, Ni,

DOI: 10.1021/acssuschemeng.6b03096
ACS Sustainable Chem. Eng. 2017, 5, 2867−2881

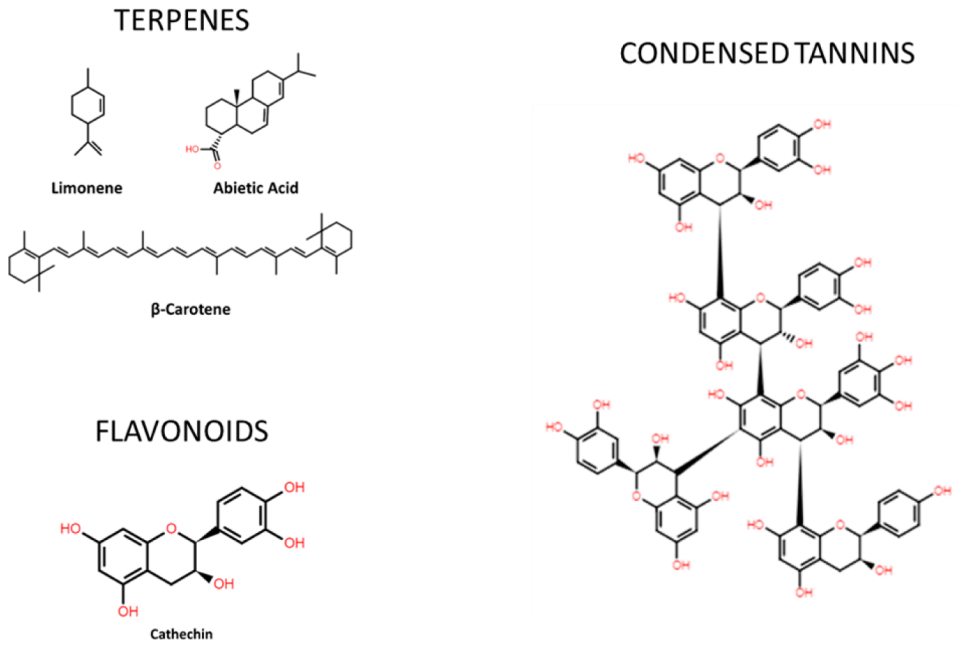

Figure 4. Typical structures of terpenes, flavonoids, and condensed tannins.

Pb, Sb, V, and Zn. With respect to coal, biomass has higher amounts of K_2O and Na_2O. The content of phosphorus oxide, especially in willow, is quite larger than in coal lignite.[36] The Catalytic Effect of Ash section briefly discusses and models the relevant catalytic effect of ash in pyrolysis process.

BIOMASS CHARACTERIZATION: REFERENCE SPECIES AND VAN KREVELEN DIAGRAM

Biomass is a complex feed and its decomposition products significantly change depending on biochemical composition. Thus, when modeling biomass pyrolysis the first step is the proper characterization of the feed with a limited number of reference species. When direct information on biochemical composition is unavailable, this composition can be derived from the elemental analysis.[8,9] The H/C/O atomic balances allow to evaluate a suitable combination of a few reference species. Cellulose, hemicellulose, lignin, and extractives constitute the largest portion of the biomass, and these are the reference species. Together with cellulose and hemicellulose, three different lignins, rich in carbon, hydrogen and oxygen, are considered as reference species. Wood plants have higher cellulose/hemicellulose ratios with respect to grasses and cereals. Lignins are less abundant in cereals with respect to woods, whereas extractives are more abundant in grasses.[9] Two further lumped species account for hydrophobic (TGL) and hydrophilic (TANN) extractives. Figure S4 reports structure and formula of the seven reference species.

Figure 5 shows the van Krevelen diagram,[37] where the composition of the different lignins of Table S1 are reported in terms of atomic H/C and O/C ratios.[30] They can be considered as a linear combination of the three reference lignins, respecting the atomic H/C/O balances. Lignin samples, which lie outside the triangle of the three reference lignins, are characterized by including small amounts of extractives or holocellulose. LIG-O is more abundant in hardwoods, whereas LIG-C is more present in softwoods. This fact well agrees with the dominant presence of syringyl propanoid units in hardwood species.

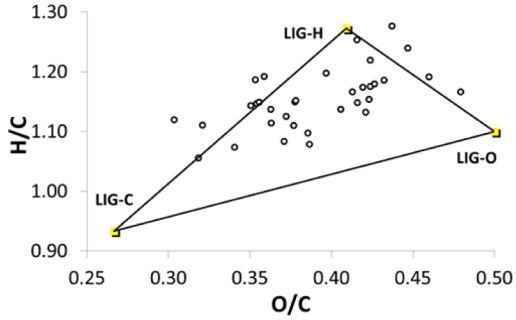

Figure 5. Composition of typical lignin samples and reference species.

In a similar way, Figure 6 shows the seven reference species in the van Krevelen diagram, together with samples of the biomass database. Three reference mixtures (RM-1, RM-2, and RM-3) are first defined as different combinations of the seven reference species, in order to reduce the number of freedom degrees. RM-1 is representative of holocellulose, whereas RM-2 and RM-3 are mixtures of lignins with some content of

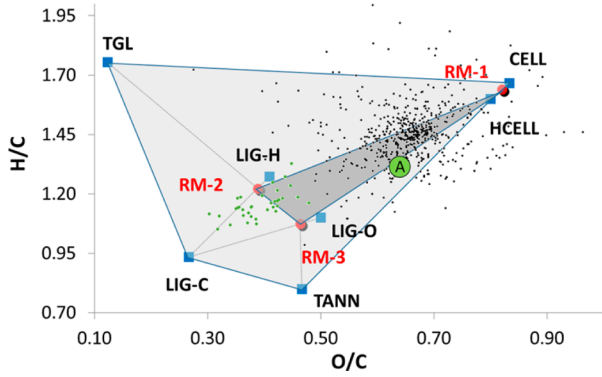

Figure 6. Biomass characterization. Reference species and several biomass samples in the H/C vs O/C van Krevelen diagram. A refers to a hybrid poplar sample (see text).

DOI: 10.1021/acssuschemeng.6b03096
ACS Sustainable Chem. Eng. 2017, 5, 2867−2881

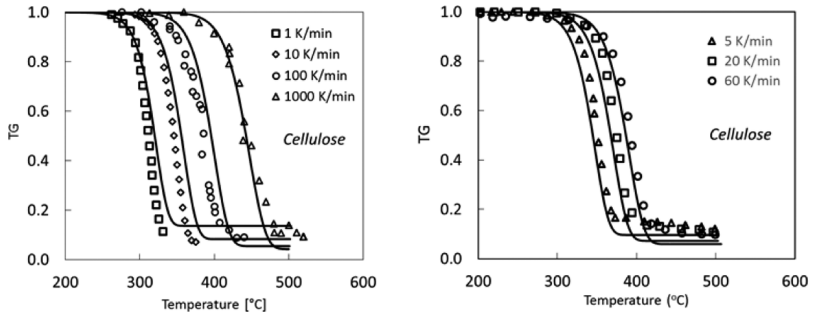

Figure 7. Pyrolysis of cellulose. (Left Panel): TGA at 1 and 10 °C/min,[54] 100 and 1000 °C/min.[55] (Right Panel): TGA at 5, 20, and 60 K/min.[53]

extractives. The internal composition of these mixtures are defined from experimental findings and can be easily modified. The C/H/O mass balances first allow to evaluate the relative content of the three reference mixtures. The amount of the seven reference components is then derived from the internal composition of the reference mixtures.[9] A simple example is useful to explain this characterization procedure. The hybrid poplar, whose elemental mass composition is H/C/O = 0.057/0.509/0.434 (reported as A in Figure 6), is characterized including 20% TANN in RM-3. The linear system of H/C/O balance equations first gives the mass composition of the reference mixtures:

RM-1 = 0.5597 RM-2 = 0.0020 RM-3 = 0.4384

The reference mixture RM-2 is only present in a very limited amount because of the low hydrogen content, and RM-1 and RM-3 are major constituents of this biomass. From these values and the internal composition of the reference mixtures, the following mass amounts of the seven reference species are obtained:

CELL = 0.3627 HCELL = 0.1970

LIGH = 0.0017 LIGO = 0.3181 LIGC = 0.0489

TGL = 0.0000 TANN = 0.0716

Linear combinations of the seven reference species are able to describe all the biomasses contained in the shadow area of Figure 6, and this characterization procedure is able to process most of the biomasses contained in the database.

MULTISTEP KINETIC MECHANISM OF BIOMASS REFERENCE SPECIES

Once the biomass feed is characterized as a combination of reference species, the kinetic modeling of biomass pyrolysis requires the description of the different decomposition mechanisms. A common assumption and simplification is that each reference component decomposes independently through a multistep, branched mechanism of first-order reactions.[8,38−40] These apparent reactions model the release of tars and permanent gases together with the formation of residual char and ash. The multistep kinetic model here discussed is based on lumped reactions,[8] whose kinetic parameters and stoichiometries were derived from experimental findings and progressively extended and updated, based on new experimental data. Experiments on temperature profiles in thick particles allowed us to validate better the endothermic tar release and the exothermic charring process.[41] A peculiarity of this model is a detailed characterization of released pyrolysis products, including not only water vapor and permanent gases (H_2, CO, CO_2, CH_4, and C_2H_4), several alcohols, aldehydes, and carbonyl compounds but also different sugars together with heterocyclic and phenolic components. At high temperatures, several chemisorbed species contribute to describe the successive steps of char devolatilization with the progressive release of H_2, CO, and CO_2.

Cellulose. On the basis of thermogravimetric studies, Broido and Shafizadeh developed the first global kinetic scheme of cellulose pyrolysis,[42,43] considering two parallel reactions forming tars, char and gases. The generally used and accepted Broido−Shafizadeh kinetic model (B−S model) considers the formation of an intermediate, active cellulose, which then decomposes into gases, tars, and char,[44] as shown in Figure S5. Cellulose pyrolysis mechanism is characterized by a first depolymerization step producing active cellulose with an apparent activation energy of 47 kcal/mol.[45,46] The first depolymerization reaction to form active cellulose reduces the polymerization degree without volatile release. Active cellulose then decomposes with two competitive reactions: a main reaction releasing levoglucosan and a slower decomposition to form char and permanent gases. Only at high temperatures (T > 750 K), decomposition reaction prevails over tar release. A side charring and exothermic reaction is also considered. This lumped multistep kinetic mechanism is reported in Table 1, and roughly simplifies the complex nature and the concerted mechanisms of cellulose decomposition.[47,48] Several intermediate species, here reported as G{·}, are first trapped in the metaplastic phase, and only then released to the gas phase.

Broadbelt's team extensively studied, from a theoretical and experimental viewpoint, the fast pyrolysis of neat glucose-based carbohydrates and also developed a detailed mechanistic model involving about 100 species and 300 reactions.[49,50] Similarly, Seshadri and Westmoreland[48,51] highlighted the implications of concerted molecular reactions for cellulose and hemicellulose kinetics, also investigating the role of hydroxyls in catalytic and noncatalytic formation of levoglucosan from glucose.

The global stoichiometry of active cellulose decomposition to form lighter products accounts for the previous mechanistic studies, and further experimental and theoretical works.[50,52,53] Thus, the lumped reactions to form hydroxyl-acetaldehyde, glyoxal, acetone, hydroxy-acetone, furfural, and 5-hydroxymethyl-furfural, together with lighter products such as formaldehyde, formic acid, CO, and CO_2 can be partially justified on mechanistic basis. Although the tar release is an endothermic process and it absorbs ∼500 kJ/kg, the char formation is an exothermic process releasing ∼2000 kJ/kg of char formed.[41] Figure 7 shows a few comparisons between model predictions and experimental data of TGA of isolated cellulose at different heating rates from 1 up to 1000 K/min.[53−55] Model predictions agree with experiments, within the experimental uncertainties.

DOI: 10.1021/acssuschemeng.6b03096
ACS Sustainable Chem. Eng. 2017, 5, 2867−2881

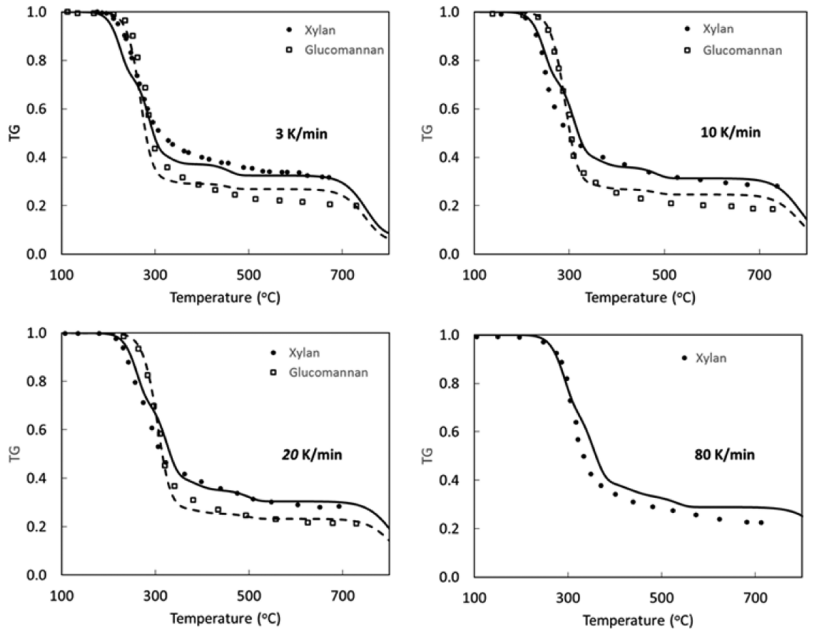

Figure 8. Pyrolysis of Hemicellulose: thermogravimetric analysis of xylan and glucomannan at 3, 10, 20, and 80 K/min. Comparisons between model predictions (lines) and average experimental data (symbols).[61−70]

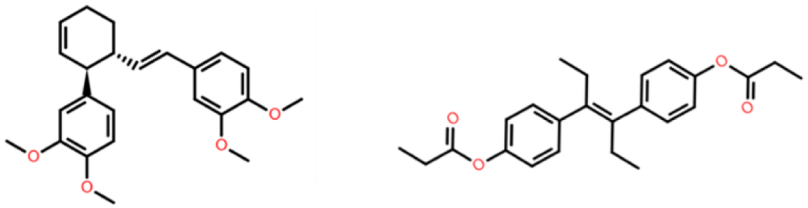

Figure 9. Heavy molecular weight lignin (HMWL). Lumped components $C_{24}H_{28}O_4$.

They are slightly slower for the first set of comparisons, whereas the remaining data show an opposite deviation.

As a further complicating aspect of fast pyrolysis, active cellulose can be ejected as high molecular weight aerosols, mainly consisting of levoglucosan, cellobiosan, and oligomers, together with other liquids formed inside the biomass sample.[46,56] Recently, Zhou et al.[57] studied the significant catalytic effect of NaCl on levoglucosan pyrolysis; this effect will be analyzed in the Catalytic Effect of Ash section.

Hemicellulose. The sugar units of hemicellulose mainly consist of homopolymers (xylans), or heteropolymers (glucomannans). Many of the OH-groups at C2 and C3 of the xylanpyranosyl units are substituted by O-acetyl groups. Several units are often side groups of the main chain (e.g., 4-*O*-methylglucuronic acid, galactose). The average degree of polymerization of hemicellulose is lower than that of cellulose, leading to a relatively faster decomposition process. Hemicellulose structures are largely different in hardwood and softwood. Whereas glucomannans are abundant in softwoods, xylans with a high percentage of acetyl substitutions are dominant in hardwoods.[58]

Grønli et al.[20] highlighted that hemicellulose in softwood is less reactive than in hardwood. Prins et al.[59] observed the same behavior in torrefaction experiments. Despite these differences, several studies on xylan pyrolysis are available, whereas glucomannans received limited attention.[58] Hemicellulose from hardwood is slightly more reactive, releases larger amounts of acetic acid, and shows a higher solid residue,[60] as shown in Figure S6, which compares several experimental TGA of xylans and glucomannans, at heating rates from 3 to 80 K/min.[61−70]

With respect to the original multistep kinetic model,[8,9] two different reference components are here considered in order to distinguish the different pyrolysis behavior of hardwood (XYHW) and softwood (GMSW) hemicellulose polymers. Figure S5 shows the similarities between the multistep kinetic mechanism of cellulose and hemicellulose. The two intermediate species (HCE-1 and HCE-2) initially formed reflect the different compositions of hardwood and softwood hemicellulose and they allow one to explain the higher formation of acetic acid and residual char from hardwood samples, as well as the higher volatile yields from softwoods. Main species from glucomannan pyrolysis include acetic acid, hydroxyacetaldehyde, hydroxypropanone, formic acid, and furfuryl alcohol, as recently discussed by Branca et al.[58] Hemicelluloses release together with C5 and C6 tar components, permanent gases, a wide number of oxygenated species, including formic and acetic acid, hydroxy-acetaldehyde, acetone, acetol, furfural, and 5-hydroxymethyl-furfural.[28,53] Figure 8 satisfactorily compares the average experimental TGA of xylan and glucomannan with model predictions.

Lignin. Lignin pyrolysis products largely retain the structure of original monolignols. Syringol derivatives are products derived from S-lignin units, whereas guaiacols are products derived from G-lignin units.[71] Klein and Virk[72] developed a lignin pyrolysis model based on a statistical characterization of

DOI: 10.1021/acssuschemeng.6b03096
ACS Sustainable Chem. Eng. 2017, 5, 2867−2881

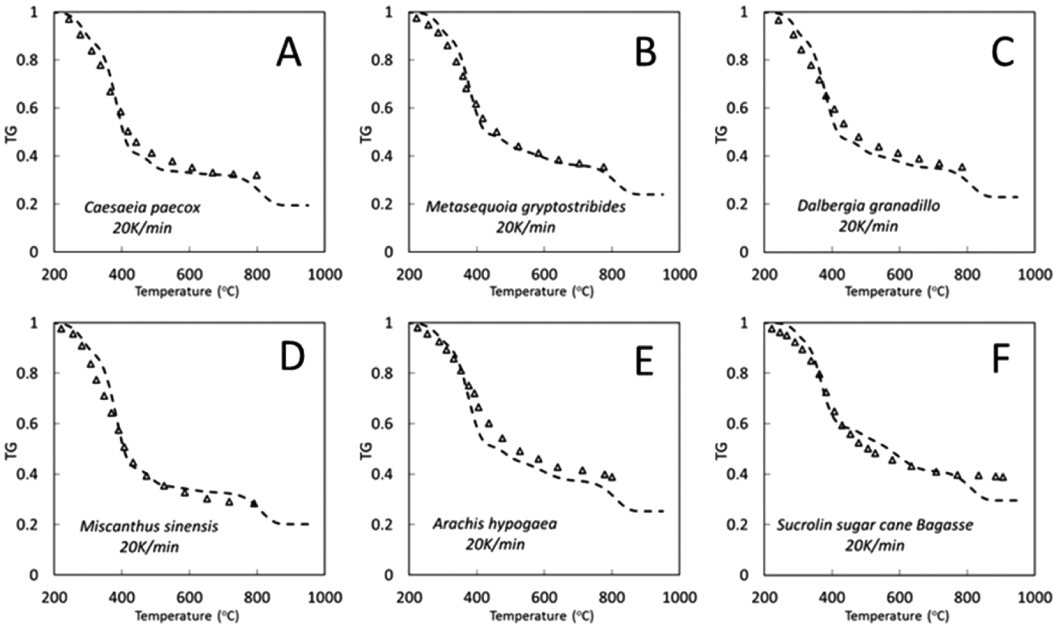

Figure 10. Lignin pyrolysis (heating rates 20 K/min). Comparisons of model predictions (lines) and experimental data (points): Panels A–E[75] and Panel F.[76]

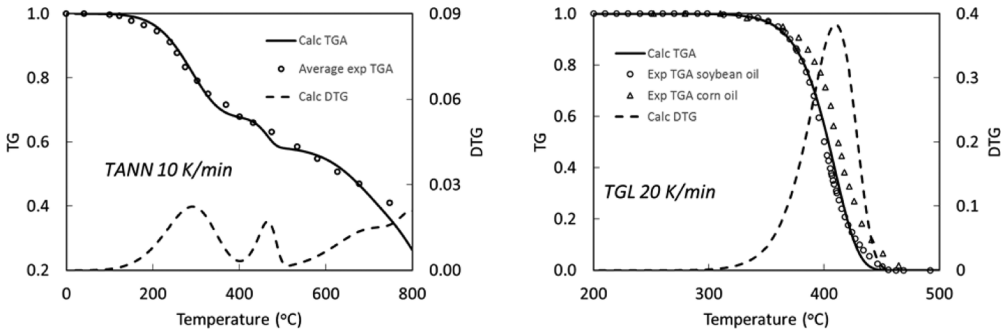

Figure 11. TGA and DTG of extractives. (Left Panel) Average data of condensed tannins.[78,82] (Right Panel) Natural vegetable oils (TGL).[83,84] Model predictions (lines) and experimental data (symbols).

the lignin structure, which is assumed as the juxtaposition of methoxy phenol and a propanoid side chain attribute on an aromatic ring. The model is able to describe lignin pyrolysis in terms of gases, water, methanol, tar species (guaiacol, catechol, and phenol), and a residual char. Yanez et al.[73] created a more complete library of lignin structures, in order to analyze hyperbranched lignin topology.

The multistep kinetic scheme of lignin decomposition here considered is a simplification of the detailed mechanism of Faravelli et al.[30] and fairly fits the one discussed by Zhou et al.,[74] as shown in Figure S7. Lignin pyrolysis reactions are active in a wide temperature range and release phenolic components. Phenol, anisole (metoxy-benzene), 2,6-dimethoxy-phenol, 4-(3-hydroxy-1-propenyl)phenol, and 3-(4-hydroxy-3,5-dimethoxy-phenyl)-acrylaldehyde are the selected lumped species representatives of these compounds. Heavy molecular weight lignins (HMWL) are also released and only one lumped component $C_{24}H_{28}O_4$ is here considered. Figure 9 shows the *trans*-3-(3,4-dimethoxyphenyl)-4-((E)-3,4-dimethoxystyryl)-cyclohex-1-ene and the diethylstilbestrol-dipropionate as a couple of possible representative components. Figure 10 compares model predictions and experimental TGA of different lignins, at heating rates of 20 K/min.[75−77] Observed deviations are within the experimental uncertainties, mainly when considering that lignins were extracted with different methods, which can affect both thermal behavior and lignin properties.[17]

Extractives. Several experimental data contributed to the definition of the two step kinetic mechanism of tannin (TANN) decomposition reported in Table 1. Relevant amounts of phenol and catechol species are released in the pyrolysis process at 300−400 °C, then there is a slow cross-linking and charification process followed by a further peak in the DTG curve at high temperatures.[78] A polymeric intermediate (ITANN: $C_8H_4O_4$, 3,5-dihydroxy-benzofuranone) is the lumped species involved in the charification reactions. Figure 11 compares model predictions and the average of several experimental data of TGA of condensed tannins, at TG 10 °C/min under nitrogen.[78−82]

Soybean and corn oil TGAs are useful to define the kinetic mechanism of resins and triglycerides (TGL) pyrolysis. As shown in Table 1, TGL devolatilization is assumed as a single step kinetics releasing acrolein (C_2H_3CHO) together with two fatty acids and one aldehyde, without significant residue. The lumped species (FFA: $C_{18}H_{32}O_2$) represents a mixture of free fatty acids. The right panel of Figure 11 shows a satisfactory

DOI: 10.1021/acssuschemeng.6b03096
ACS Sustainable Chem. Eng. 2017, 5, 2867−2881

Table 1. Multistep Kinetic Scheme of Biomass Pyrolysis

	Pyrolysis Reactions			Kinetic Parameters A (s^{-1}), Eact
			Cellulose	
1	CELL	→	CELLA	$1.5 \times 10^{14} \times \exp(-47000/RT)$
2	CELLA	→	0.4 HAA + 0.05 GLYOX + 0.15 CH_3CHO + 0.25 HMFU + 0.35 ALD3 + 0.15 CH_3OH + 0.3 CH_2O + 0.61 CO + 0.36 CO_2 + 0.05 H_2 + 0.93 H_2O + 0.02 HCOOH + 0.05 $C_3H_6O_2$ + 0.05 G{CH_4}+	$2.5 \times 10^{6} \times \exp(-19100/RT)$
3	CELLA	→	LVG	$3.3 \times T \times \exp(-10000/RT)$
4	CELL	→	5 H_2O + 6 CHAR	$6 \times 10^{7} \times \exp(-31000/RT)$
			Hemicellulose	
5	GMSW	→	0.70 HCE1 + 0.30 HCE2	$1 \times 10^{10} \times \exp(-31000/RT)$
6	XYHW	→	0.35 HCE1 + 0.65 HCE2	$1 \times 10^{10} \times \exp(-28500/RT)$
7	HCE1	→	0.6 XYLAN + 0.2 $C_3H_6O_2$ + 0.12 GLYOX + 0.2 FURF + 0.4 H_2O + 0.08 G{H_2} + 0.16 CO	$3 \times T \times \exp(-11000/RT)$
8	HCE1	→	0.4 H_2O + 0.79 CO_2 + 0.05 HCOOH + 0.69 CO + 0.01 G{CO} + 0.01 G{CO_2} + 0.35 G{H_2} + 0.3 CH_2O + 0.9 G{COH_2} + 0.625 G{CH_4} + 0.375 G{C_2H_4} + 0.875 CHAR	$1.8 \times 10^{-3} \times T \times \exp(-3000/RT)$
9	HCE2	→	0.2 H_2O + 0.275 CO + 0.275 CO_2 + 0.4 CH_2O + 0.1 C_2H_5OH + 0.05 HAA + 0.35ACAC + 0.025 HCOOH + 0.25 G{CH_4} + 0.3 G{CH_3OH} + 0.225 G{C_2H_4} + 0.4 G{CO_2} + 0.725 G{COH_2}+	$5 \times 10^{9} \times \exp(-31500/RT)$
			Lignins	
10	LIGC	→	0.35 LIGCC + 0.1 COUMARYL + 0.08 PHENOL + 0.41 C_2H_4 + 1.0H_2O + 0.7 G{COH_2} + 0.3 CH_2O + 0.32 CO + 0.495 G{CH_4}+	$1 \times 10^{11} \times \exp(-37200/RT)$
11	LIGH	→	LIGOH + 0.5 ALD3 + 0.5 C_2H_4 + 0.2 HAA + 0.1 CO + 0.1 G{H_2}	$6.7 \times 10^{12} \times \exp(-37500/RT)$
12	LIGO	→	LIGOH + CO_2	$3.3 \times 10^{8} \times \exp(-25500/RT)$
13	LIGCC	→	0.3 COUMARYL + 0.2 PHENOL + 0.35 HAA + 0.7 H_2O + 0.65 CH_4 + 0.6 C_2H_4 + H_2 + 1.4 CO + 0.4 G{CO} + 6.75 CHAR	$1 \times 10^{4} \times \exp(-24800/RT)$
14	LIGOH	→	0.9 LIG + H_2O + 0.1 CH_4 + 0.6 CH_3OH + 0.05 G{H_2} + 0.3 G{CH_3OH} + 0.05 CO_2 + 0.65 CO + 0.6 G{CO} + 0.05 HCOOH + 0.85 G{COH_2} + 0.35 G{CH_4} + 0.2 G{C_2H_4} + 4.25 CHAR+	$1 \times 10^{8} \times \exp(-30000/RT)$
15	LIG	→	0.7 FE2MACR + 0.3 ANISOLE + 0.3 CO + 0.3 G{CO} + 0.3 CH_3CHO	$4 \times T \times \exp(-12000/RT)$
16	LIG	→	0.6 H_2O + 0.4 CO + 0.2 CH_4 + 0.4 CH_2O + 0.2 G{CO} + 0.4 G{CH_4} + 0.5 G{C_2H_4} + 0.4 G{CH_3OH} + 2 G{COH_2} + 6 CHAR	$8.3 \times 10^{-2} \times T \times \exp(-8000/RT)$
17	LIG	→	0.6 H_2O + 2.6 CO + 1.1 CH_4 + 0.4 CH_2O + C_2H_4 + 0.4 CH_3OH+	$1 \times 10^{7} \times \exp(-24300/RT)$
			Extractives	
18	TGL	→	ACROL + 3 FFA	$7 \times 10^{12} \times \exp(-45700/RT)$
19	TANN	→	0.85 FENOL + 0.15 G{PHENOL} + G{CO} + H_2O + ITANN	$2 \times 10^{1} \times \exp(-10000/RT)$
20	ITANN	→	5 CHAR + 2 CO + H_2O + G{COH_2}	$1 \times 10^{3} \times \exp(-25000/RT)$
			Metaplastic	
21	G{CO_2}	→	CO_2	$1 \times 10^{6} \times \exp(-24000/RT)$
22	G{CO}	→	CO	$5 \times 10^{12} \times \exp(-50000/RT)$
23	G{COH_2}	→	CO + H_2	$1.5 \times 10^{12} \times \exp(-71000/RT)$
24	G{H_2}	→	H_2	$5 \times 10^{11} \times \exp(-75000/RT)$
25	G{CH_4}	→	CH_4	$5 \times 10^{12} \times \exp(-71500/RT)$
26	G{CH_3OH}	→	CH_3OH	$2 \times 10^{12} \times \exp(-50000/RT)$
27	G{C_2H_4}	→	C_2H_4	$5 \times 10^{12} \times \exp(-71500/RT)$
28	G{PHENOL}	→	PHENOL	$1.5 \times 10^{12} \times \exp(-71000/RT)$
			H_2O Evap.	
29	ACQUA	→	H_2O	$1 \times T \times \exp(-8000/RT)$

comparison between model predictions and experimental TGA at 20 K/min.[83,84]

BIOMASS PYROLYSIS AND RELEASED PRODUCTS

As already mentioned, biomass is characterized as a mixture of reference components, which decompose independently through the lumped kinetic mechanisms of Table 1. The common assumption is that biomass pyrolysis products are derived as a linear combination of the pyrolysis products of the reference species. Of course, these assumptions and lumping rules limit the correctness and accuracy of the model, but they constitute a reasonable compromise. As it will be better discussed in the conclusion of this work, all these simplifications can be easily modified and revised in order further improve the model and/or to account for new experimental information.

All these simplifications aim at an effective use not only at the particle but also at the reactor scale. Computational time limitations are indeed very severe when simulating a reactor device considering transport limitations and secondary gas-phase reactions.[7,11,85]

Thus, biomass is characterized as a mixture of the seven reference components, whose internal composition either is obtained through the biochemical analysis, or is derived from elemental analysis. A couple of examples are useful to describe how to characterize different biomass samples.

A first example refers to *Pinus radiata* sawdust,[77] whose biochemical composition determined with NMR, was 55.5 of holocellulose, 32.8 of lignin, 5.8 of extractives, together with 5.24 of moisture and 0.7 of ash. According to typical internal ratios, holocellulose is considered as 75% of cellulose and 25% of softwood hemicellulose (glucomannans). Moreover, lignin is divided into 80% of LIG-O and 20% LIG-C, whereas extractives

DOI: 10.1021/acssuschemeng.6b03096
ACS Sustainable Chem. Eng. 2017, 5, 2867−2881

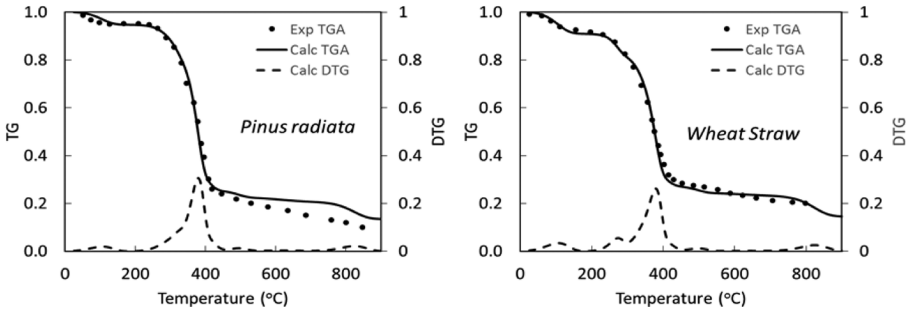

Figure 12. TGAs of *Pinus radiata*[77] and Wheat Straw[86] at heating rate of 80 K/min. Comparisons of predicted (lines) and experimental (symbols).

are tannins, due to the high oxygen content of this biomass. The biomass is then characterized in the following way:

CELL = 0.419 HCELL = 0.140 (glucomannans)

LIGH = 0.0 LIGO = 0.262 LIGC = 0.066

TGL = 0.0 TANN = 0.052 Moisture = 0.052

ASH = 0.007

A second characterization example refers to a wheat straw sample, where only the elemental composition is given (C/H/O = 49.3/5.7/45.0 wt).[86] The three reference mixtures are first defined. RM1 is the holocellulose with a molar ratio cellulose/hemicellulose =1.33, being a hardwood biomass. Reference mixtures RM-2 and RM-3 are mixtures of the three different lignins, with extractives.[9] Because of the relatively low H content of this biomass, a linear combination 68% of RM-1 and 32% of RM-3 satisfies the elemental biomass composition. By splitting the reference mixtures, the biomass composition becomes

CELL = 0.373 HCELL = 0.230 (xylans)

LIGH = 0.0 LIGO = 0.164 LIGC = 0.025

TANN = 0.099

Finally, moisture and ash are 9 and 1.9%, respectively.

Figure 12 shows the comparisons of predicted and experimental TGAs of these biomasses at a heating rate of 80 K/min together with the differential (DTG) curves. They clearly show the peak of cellulose devolatilization at ∼400 °C and a shoulder before cellulose peak, more pronounced for wheat straw, due to the thermal behavior of xylan hemicellulose.

Table 2 compares the predicted volatile species released from the pyrolysis of the two samples at 700 °C and 80 K/min. The amount and the H/C/O composition of the solid residue is also reported. Levoglucosan (LVG) is the most abundant volatile species for both samples, because of the large cellulose amount. The possible LVG degradation both for the catalytic effect of ash and for sample size will be discussed later. Together with phenol, only a few species (anisole, coumaryl alcohol, synapyl aldehyde, and HMWL) lump phenolic derivatives, and they are more abundant from the pyrolysis of pine sawdust, because of greater amount of lignins. Comparisons of model predictions with experimental data are only partial and difficult, not only for the limited availability of reliable measurements, but mainly for effect of secondary gas phase reactions of released products. Because of the moderate final temperature, still there is ∼20−25 wt % of oxygen and ∼4−5 wt % of hydrogen in the predicted residual char.

The products reported in Table 2 represent the set of volatile species released by the biomass pyrolysis kinetic scheme reported in Table 1. These volatile species, once released in the gas phase can undergo successive decomposition and oxidation reactions. Table S2 reports the formation enthalpy ($\Delta H_{f,298}$) and entropy ($\Delta S_{f,298}$) of major oxygenated species released from biomass pyrolysis. Successive gas phase reactions of all these species are considered in the POLIMI kinetic mechanism, and are discussed in Note II of this work.[11]

It is evident that the lumped kinetic mechanism of Table 1 can be improved in terms of new reaction steps, kinetic parameters, and reaction stoichiometries.[21] Moreover, the interactions among reference species are not considered. Cellulose and lignin interactions during fast pyrolysis seem to inhibit levoglucosan formation due to their inherent covalent linkages.[87] New theoretical and experimental studies on biomass pyrolysis,[53] as well as new analytical techniques[88] allow extensions and improvements of the overall mechanism. Ashes can catalyze and significantly modify the biomass pyrolysis products[89] and next Section addresses these effects.

Catalytic Effect of Ash. The catalytic effect of ashes during fast pyrolysis typically decreases bio-oil selectivity. In fact, while pyrolysis products form, they can interact with inorganic elements in the residual solid. Particularly, levoglucosan reacts on minerals of residual char, forming levoglucosenone, furan derivatives, and lighter oxygenates such as acetic acid, acetone, and acetol.[71] Demineralization and pretreatments of biomass with water and acidic solutions in order to reduce ash content decreases the catalytic effects of inorganic salts.[90]

Different inorganics are responsible for different types of secondary reactions.[91] Metal cations favors the homolytic cleavage of pyranose ring bonds over the heterolytic cleavage of glycosidic linkages, favoring the formation of light oxygenates at the expense of levoglucosan. The following reactivity trend is observed with respect to levoglucosan reduction:[92]

K > Na > Ca > Mg

Although all these cations catalyze levoglucosan decomposition, Na and K mainly favor the formation of formic acid, glycolaldehyde, and acetol, whereas Mg and Ca promote dehydration reactions and furfural formation.[71] Similar effects are observed on xylan pyrolysis, whereas there is a negligible effect of inorganics on the pyrolysis behavior of lignin fraction. Very recently, Zhou et al.[57] deeply investigated the catalytic effects of NaCl on fast pyrolysis of carbohydrates. Levoglucosan sharp reduction was mainly caused by the catalytic effect of Na on the competing dehydration reactions. Zhu et al.[93] studied the catalytic effect of alkaline earth metals on cellulose pyrolysis. Ca ions are more active than Mg ions and they promote the primary formation of char from cellulose, the

DOI: 10.1021/acssuschemeng.6b03096
ACS Sustainable Chem. Eng. 2017, 5, 2867−2881

Table 2. Pyrolysis of *Pinus radiata* and Wheat Straw at 80 K/min; Characterization in Terms of Reference Species and Predicted Composition of Primary Pyrolysis Products and Residual Char, at 700 °C

	Pine Sawdust	Wheat Straw
Temperature (°C)	700	700
Heating Rate (K/min)	80	80
Biomass Characterization (wt %)		
CELL	41.7	37.3
HCELL	13.9	23.0
LIG (LIGH+LIGO+LIGC)	32.6	18.9
TANN	6.0	9.9
TGL	0.0	0.0
MOISTURE	5.2	9.0
ASH	0.7	1.9
Gases (wt % of initial biomass)	13.9	13.3
CO	6.4	5.6
CO_2	6.2	7.1
H_2	0.0	0.0
C_2H_4	0.8	0.4
CH_4	0.5	0.3
Condensables (wt % of initial biomass)	65.6	64.5
H_2O	11.5	14.5
CH_2O	2.3	2.9
CH_3OH	2.9	2.8
CH_3CHO	0.8	0.6
HCOOH	0.3	0.3
C_2H_5OH	0.2	0.5
Acrolein	0.3	0.2
Glyoxal	0.8	0.7
Hydroxy-acetaldehyde	3.0	2.8
Acetic Acid	0.8	2.4
Propanal/Acetone	1.7	1.6
Acetol ($C_3H_6O_2$)	1.8	1.5
Furfural	0.9	0.7
C_5 Sugars	4.7	3.7
Phenol	1.9	2.7
Hydroxy-methyl-furfural	3.2	2.8
Levoglucosan	22.0	19.7
Anisole	1.0	0.6
Coumaryl Alcohol	0.7	0.3
Sinapyl Aldehyde	4.3	2.7
Heavy Mol. Weight Lignin (HMWL)	0.6	0.4
Solid Residue (wt % of initial biomass)	20.3	21.7
CHAR	19.6	19.8
C	77.1	70.9
H	4.1	4.7
O	18.9	24.3
ASH	0.7	1.9

conversion of levoglucosan to light oxygenates and furans, and the successive decomposition of furans to char and permanent gases.

Figure 13 shows the yields of bio-oil from fast biomass pyrolysis, as obtained in the VTT's 20 kg/h pyrolyzer.[94] Higher ash content leads to lower oil yield, and to bio-oils with higher water content. This confirms the catalytic effect of ash promoting pyrolysis and dehydration reactions, decreasing bio-oil yield.

Trendewicz et al.[89] already proposed a modification of the cellulose mechanism of Table 1 in order to include K effect on pyrolysis products. On the basis of pyrolysis experiments of

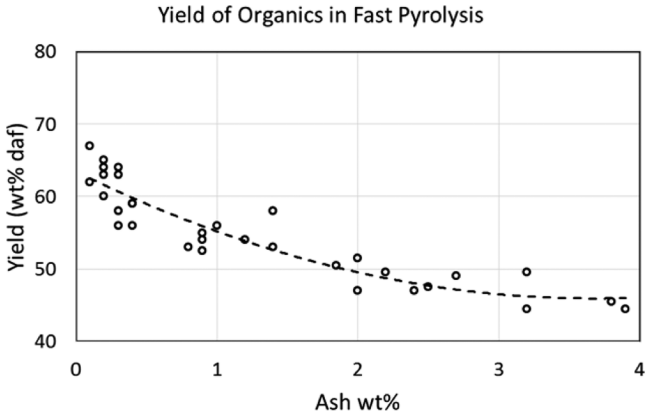

Figure 13. Effect of ash content on the yields of bio-oil from fast pyrolysis of biomass in the VTT pyrolyzer.[94]

cellulose samples treated with different K levels (0−1% mass fraction), they changed the kinetic parameters. To maintain a flexible and simple mechanism, we prefer to modify the kinetic parameters of a few selected reactions of Table 1, based on a single ash parameter. The major catalytic effect of ash is the reduction of levoglucosan and xylan in favor of decomposition and dehydration products, along with a char increase. Two splitting or selectivity parameters govern the product distribution of cellulose decomposition (see Figure SM_5). The first one (S_1) refers to the selectivity toward active cellulose, whereas the second one (S_2) is the selectivity of levoglucosan released by active cellulose. Figure 14 shows how these selectivities vary as a function of reaction temperature. These are average selectivities, as obtained from the kinetic parameters reported in Table 1. The ash catalytic effect is to reduce both these selectivities.

Let us now define for the different biomass samples a global ash factor (AF) in adimensional form, with values ranging between 0 (no ash) and 1 (more than 5 wt %). It is assumed that catalytic effect is already completed for ash content of 5 wt %. It is then possible to define AF as a function of the ash content (wt %) with the following expression:

$$\mathrm{AF} = \tanh(\mathrm{ash}/2)$$

The ash factor ranges from zero (low ash content) to asymptotically 1 (ash content higher than 4−5%), and it assumes a value of about 0.5 for ash content in the order of 1 wt %.

The right panel of Figure 14 shows the modified selectivities for biomass samples without ash, and with the maximum ash content. These corrections are obtained by simply modifying the activation energy of the decomposition reaction of active cellulose (E_2) and the activation energy of the charification reaction (E_4) as a function of the ash factor (AF):

$$E_2 = 19100 - 600x(\mathrm{AF} - 0.5)\ [\mathrm{kcal/kmol}]$$

$$E_4 = 31000 - 1000x(\mathrm{AF} - 0.5)\ [\mathrm{kcal/kmol}]$$

The reference kinetic parameters reported in Table 1 refer to an average biomass sample, i.e., an average ash content of 1 wt % (AF = 0.5). Similarly, the decomposition reaction of hemicellulose intermediate (HCE1) is favored in the presence of high ash content and the activation energy of the corresponding decomposition reaction becomes

$$E_8 = 3000 - 1000x(\mathrm{AF} - 0.5)\ [\mathrm{kcal/kmol}]$$

DOI: 10.1021/acssuschemeng.6b03096
ACS Sustainable Chem. Eng. 2017, 5, 2867−2881

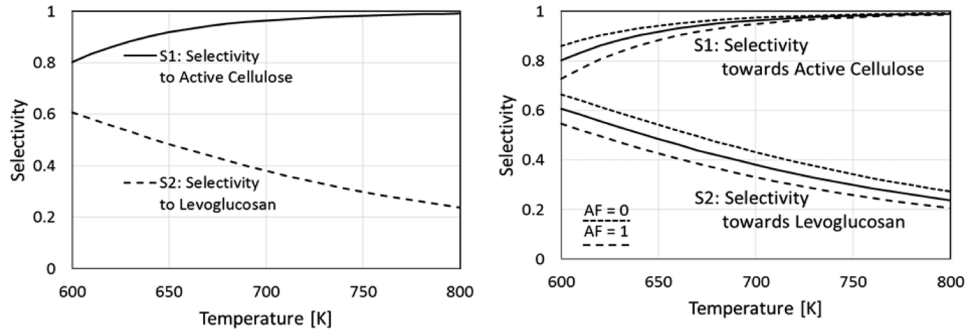

Figure 14. Cellulose Pyrolysis: (Left Panel) Average selectivity toward active cellulose and levoglucosan as a function of the reaction temperature. (Right Panel) Effect of ash on active cellulose and levoglucosan selectivity. Solid lines refer to the kinetic scheme of Table 1 (AF = 0.5).

It is evident that these corrections are strongly simplified, but they account for the major catalytic effect of ash.

An insightful analysis of Figure 14 is useful for an evaluation of the global effect of the ash factor on the oil yields of Figure 13. The catalytic effect of ash is in the order of at least 10 kg of organics per 100 kg of biomass, on daf basis. At 650−700 K, Figure 14 shows that the presence of ash reduces the selectivity toward active cellulose (first precursor of bio-oil) of 4−6%. This is a first reason for higher residual char and lower yields of organics. Moreover, the ash decreases the selectivity of active cellulose toward levoglucosan of more than 10%. A similar ash effect and reduction of xylan yields is also predicted from hemicellulose pyrolysis. Based on a typical value of 65−70% of holocellulose in the fresh biomass, the predicted differences between samples with and without ashes properly sum up to about 10%.

CONCLUSION

This work discusses the first steps of a comprehensive and unifying mathematical model to describe the fast pyrolysis of biomass particles. Based on elemental analysis, biomass samples are characterized in terms of a few reference components, whose pyrolysis mechanism is described with lumped kinetic models. The satisfactory comparisons with several experimental data prove the model reliability. Although the model validation is here limited to thermogravimetric analysis of reference species and a couple of biomass samples, extensive comparisons with product compositions are reported in the previous referred papers,[7,8,41] as well as in Note II of this work.[11]

Since the original formulation,[8] the characterization model has been progressively extended to include extractive components,[9] and here is further improved to account for the differences between hardwood and softwood biomass samples. This different composition allows to explain the higher volatile yields from softwood, as well as the higher formation of acetic acid and residual char from hardwood samples. The pyrolysis mechanism of lignins has been revised with the introduction of a new lumped component to represent heavy molecular weight lignins. Finally, a further extension and refinement of the kinetic mechanism regards the reduction of the oil yields, because of the catalytic effect of inorganic elements.[87]

It is relevant to underline that this lumped biomass pyrolysis mechanism remains a rough attempt to describe the complex behavior of pyrolysis products. The rate parameters and stoichiometries reported in Table 1 summarize the comparisons of model predictions with several experimental data. The simplified approach applied to describe ash effect with the single AF parameter is a further example of the possibilities to improve the overall kinetic model. For instance, the distinction among the catalytic effects of Na/K and Ca/Mg can be included by adding one or more apparent dehydration and decomposition reactions.[95] Similarly, the effect of particle sizes with heterogeneous reactions and secondary char formation could deserve particular attention, especially for large biomass particles. A further possible factor affecting the yield of pyrolysis bio-oil also includes the interaction between cellulose and lignin. In fact, this interaction during fast pyrolysis can inhibit the formation of levoglucosan due to the inherent covalent linkages between cellulose and lignin.[90,96]

Biomass characterization and pyrolysis are only the first steps in the modeling of fast biomass pyrolysis. Note II of this work[11] analyzes the gasification reactions of residual char and secondary gas-phase reactions of pyrolysis products, together with the coupling of kinetics and transport resistances at particle and reactor scale. Only in this way, the overall model can predict bio-oil formation from fast pyrolysis processes.

ASSOCIATED CONTENT

Supporting Information

The Supporting Information is available free of charge on the ACS Publications website at DOI: 10.1021/acssuschemeng.6b03096.

Further information on biomass structure and biomass pyrolysis mechanism; formation enthalpy and entropy of major oxygenated species released from biomass pyrolysis (PDF)

AUTHOR INFORMATION

Corresponding Author

*E. Ranzi. Phone: +39 (0)2 2399 3250; Fax: +39 (0)2 7063 8173; Email: eliseo.ranzi@polimi.it.

ORCID

Eliseo Ranzi: 0000-0002-1395-6074

Notes

The authors declare no competing financial interest.

ACKNOWLEDGMENTS

P.D. gratefully acknowledges the financial support from CAPES Foundation, Ministry of Education of Brazil−Science without Borders Mobility Program−Full PhD Scholarship Process No. 10131/13-2. This paper summarizes the research activities on biomass pyrolysis done at CMIC Department of Politecnico di Milano. The contributions of all the friends, colleagues, and Ph.D. and Master students are gratefully acknowledged.

DOI: 10.1021/acssuschemeng.6b03096
ACS Sustainable Chem. Eng. 2017, 5, 2867−2881

Particularly, the authors acknowledge the very useful works, discussions, and comments of Prof. M. Dente, S. Pierucci, T. Faravelli, A. Cuoci, and F. Manenti.

REFERENCES

(1) Bridgwater, A. V. Review of fast pyrolysis of biomass and product upgrading. *Biomass Bioenergy* **2012**, *38*, 68−94.
(2) Lehto, J.; Oasmaa, A.; Solantausta, Y.; Kytö, M.; Chiaramonti, D. Review of fuel oil quality and combustion of fast pyrolysis bio-oils from lignocellulosic biomass. *Appl. Energy* **2014**, *116*, 178−190.
(3) Olah, G. A.; Goeppert, A.; Prakash, G. S. *Beyond oil and gas: the methanol economy*; John Wiley & Sons: Hoboken, NJ, 2011.
(4) Arena, U. Process and technological aspects of municipal solid waste gasification. A review. *Waste Manage.* **2012**, *32* (4), 625−639.
(5) Leckner, B. Process aspects in combustion and gasification. Waste-to-Energy (WtE) units. *Waste Manage.* **2015**, *37*, 13−25.
(6) Mettler, M. S.; Vlachos, D. G.; Dauenhauer, P. J. Top ten fundamental challenges of biomass pyrolysis for biofuels. *Energy Environ. Sci.* **2012**, *5*, 7797−7809.
(7) Ranzi, E.; Corbetta, M.; Manenti, F.; Pierucci, S. Kinetic modeling of the thermal degradation and combustion of biomass. *Chem. Eng. Sci.* **2014**, *110*, 2−12.
(8) Ranzi, E.; Cuoci, A.; Faravelli, T.; Frassoldati, A.; Migliavacca, G.; Pierucci, S.; Sommariva, S. Chemical kinetics of biomass pyrolysis. *Energy Fuels* **2008**, *22* (6), 4292−4300.
(9) Debiagi, P. E. A.; Pecchi, C.; Gentile, G.; Frassoldati, A.; Cuoci, A.; Faravelli, T.; Ranzi, E. Extractives extend the applicability of multistep kinetic scheme of biomass pyrolysis. *Energy Fuels* **2015**, *29* (10), 6544−6555.
(10) Debiagi, P. E. A.; Gentile, G.; Pelucchi, M.; Frassoldati, A.; Cuoci, A.; Faravelli, T.; Ranzi, E. Detailed kinetic mechanism of gas-phase reactions of volatiles released from biomass pyrolysis. *Biomass Bioenergy* **2016**, *93*, 60−71.
(11) Ranzi, E., Debiagi, P.E. A., Frassoldati, A. Mathematical Modeling of Fast Biomass Pyrolysis and Bio-oil Formation. Note II: Secondary Gas-Phase Reactions and Biooil Formation*ACS Sustainable Chem. Eng.* **2017**, DOI: 10.1021/acssuschemeng.6b03098.
(12) Sluiter, J. B.; Ruiz, R. O.; Scarlata, C. J.; Sluiter, A. D.; Templeton, D. W. Compositional analysis of lignocellulosic feedstocks. 1. Review and description of methods. *J. Agric. Food Chem.* **2010**, *58* (16), 9043−9053.
(13) Vaz, S., Jr Analytical techniques for the chemical analysis of plant biomass and biomass products. *Anal. Methods* **2014**, *6* (20), 8094−8105.
(14) Parikh, J.; Channiwala, S. A.; Ghosal, G. K. A correlation for calculating HHV from proximate analysis of solid fuels. *Fuel* **2005**, *84* (5), 487−494.
(15) Aiken, A. C.; DeCarlo, P. F.; Jimenez, J. L. Elemental analysis of organic species with electron ionization high-resolution mass spectrometry. *Anal. Chem.* **2007**, *79* (21), 8350−8358.
(16) Templeton, D. W.; Wolfrum, E. J.; Yen, J. H.; Sharpless, K. E. Compositional Analysis of Biomass Reference Materials: Results from an Interlaboratory Study. *BioEnergy Res.* **2016**, *9* (1), 303−314.
(17) Yang, L.; Wang, D.; Zhou, D.; Zhang, Y. Effect of different isolation methods on structure and properties of lignin from valonea of Quercus variabilis. *Int. J. Biol. Macromol.* **2016**, *85*, 417−424.
(18) Xu, F.; Yu, J.; Tesso, T.; Dowell, F.; Wang, D. Qualitative and quantitative analysis of lignocellulosic biomass using infrared techniques: a mini-review. *Appl. Energy* **2013**, *104*, 801−809.
(19) Lupoi, J. S.; Singh, S.; Simmons, B. A.; Henry, R. J. Assessment of lignocellulosic biomass using analytical spectroscopy: an evolution to high-throughput techniques. *BioEnergy Res.* **2014**, *7* (1), 1−23.
(20) Grønli, M. G.; Várhegyi, G.; Di Blasi, C. Thermogravimetric analysis and devolatilization kinetics of wood. *Ind. Eng. Chem. Res.* **2002**, *41* (17), 4201−4208.
(21) Anca-Couce, A. Reaction mechanisms and multi-scale modelling of lignocellulosic biomass pyrolysis. *Prog. Energy Combust. Sci.* **2016**, *53*, 41−79.
(22) Zhao, X.; Zhang, L.; Liu, D. Biomass recalcitrance. Part I: the chemical compositions and physical structures affecting the enzymatic hydrolysis of lignocellulose. Biofuels. *Biofuels, Bioprod. Biorefin.* **2012**, *6* (4), 465−482.
(23) O'Sullivan, A. C. Cellulose: the structure slowly unravels. *Cellulose* **1997**, *4* (3), 173−207.
(24) Himmel, M. E.; Ding, S. Y.; Johnson, D. K.; Adney, W. S.; Nimlos, M. R.; Brady, J. W.; Foust, T. D. Biomass recalcitrance: engineering plants and enzymes for biofuels production. *Science* **2007**, *315* (5813), 804−807.
(25) Wang, Z.; Pecha, B.; Westerhof, R. J. M.; Kersten, S. R. A.; Li, C. Z.; McDonald, A. G.; Garcia Perez, M. Effect of Cellulose Crystallinity on Solid/Liquid Phase Reactions Responsible for the Formation of Carbonaceous Residues during Pyrolysis. *Ind. Eng. Chem. Res.* **2014**, *53* (8), 2940.
(26) Mukarakate, C.; Mittal, A.; Ciesielski, P. N.; Budhi, S.; Thompson, L.; Iisa, K.; Nimlos, M. R.; Donohoe, B. S. Influence of Crystal Allomorph and Crystallinity on the Products and Behavior of Cellulose during Fast Pyrolysis. *ACS Sustainable Chem. Eng.* **2016**, *4* (9), 4662−4674.
(27) Ebringerová, A. Structural diversity and application potential of hemicelluloses. *Macromol. Symp.* **2005**, *232* (1), 1−12.
(28) Zhou, X.; Li, W.; Mabon, R.; Broadbelt, L. J. A Critical Review on Hemicellulose Pyrolysis. *Energy Technology* **2017**, *5*, 52−79.
(29) Dutta, S.; De, S.; Saha, B.; Alam, M. I. Advances in conversion of hemicellulosic biomass to furfural and upgrading to biofuels. *Catal. Sci. Technol.* **2012**, *2* (10), 2025−2036.
(30) Faravelli, T.; Frassoldati, A.; Migliavacca, G.; Ranzi, E. Detailed kinetic modeling of the thermal degradation of lignins. *Biomass Bioenergy* **2010**, *34* (3), 290−301.
(31) Vanholme, R.; Demedts, B.; Morreel, K.; Ralph, J.; Boerjan, W. Lignin biosynthesis and structure. *Plant Physiol.* **2010**, *153* (3), 895−905.
(32) Xu, F.; Yu, J.; Tesso, T.; Dowell, F.; Wang, D. Qualitative and quantitative analysis of lignocellulosic biomass using infrared techniques: a mini-review. *Appl. Energy* **2013**, *104*, 801−809.
(33) Hillis, W. *Wood extractives and their significance to the pulp and paper industries*; Academic Press: New York, 1962.
(34) Hernes, P.; Hedges, J. Tannin signatures of barks, needles, leaves, cones, and wood at the molecular level. *Geochim. Cosmochim. Acta* **2004**, *68* (6), 1293−1307.
(35) Tian, F. J.; Yu, J.; McKenzie, L. J.; Hayashi, J. I.; Li, C. Z. Conversion of fuel-N into HCN and NH3 during the pyrolysis and gasification in steam: a comparative study of coal and biomass. *Energy Fuels* **2007**, *21* (2), 517−521.
(36) Karampinis, E.; Vamvuka, D.; Sfakiotakis, S.; Grammelis, P.; Itskos, G.; Kakaras, E. Comparative study of combustion properties of five energy crops and Greek lignite. *Energy Fuels* **2012**, *26* (2), 869−878.
(37) van Krevelen, D. W. Graphical-statistical method for the study of structure and reaction processes of coal. *Fuel* **1950**, *29*, 269−284.
(38) Chan, W. C. R.; Kelbon, M.; Krieger, B. B. Modelling and experimental verification of physical and chemical processes during pyrolysis of a large biomass particle. *Fuel* **1985**, *64* (11), 1505−1513.
(39) Miller, R. S.; Bellan, J. A generalized biomass pyrolysis model based on superimposed cellulose, hemicellulose and liqnin kinetics. *Combust. Sci. Technol.* **1997**, *126* (1−6), 97−137.
(40) Lewis, A. D.; Fletcher, T. H. Prediction of sawdust pyrolysis yields from a flat-flame burner using the CPD model. *Energy Fuels* **2013**, *27* (2), 942−953.
(41) Corbetta, M.; Frassoldati, A.; Bennadji, H.; Smith, K.; Serapiglia, M. J.; Gauthier, G.; Melkior, T.; Ranzi, E.; Fisher, E. M. Pyrolysis of centimeter-scale woody biomass particles: Kinetic modeling and experimental validation. *Energy Fuels* **2014**, *28* (6), 3884−3898.
(42) Kilzer, F. J.; Broido, A. Speculations on nature of cellulose pyrolysis. *Pyrodynamics* **1965**, *2* (2−3), 151.
(43) Shafizadeh, F.; Fu, Y. L. Pyrolysis of cellulose. *Carbohydr. Res.* **1973**, *29* (1), 113−122.

DOI: 10.1021/acssuschemeng.6b03096
ACS Sustainable Chem. Eng. 2017, 5, 2867−2881

(44) Bradbury, A. G.; Sakai, Y.; Shafizadeh, F. A kinetic model for pyrolysis of cellulose. *J. Appl. Polym. Sci.* **1979**, *23* (11), 3271−3280.
(45) Varhegyi, G.; Jakab, E.; Antal, M. J., Jr Is the Broido-Shafizadeh model for cellulose pyrolysis true? *Energy Fuels* **1994**, *8* (6), 1345−1352.
(46) Lédé, J. Cellulose pyrolysis kinetics: An historical review on the existence and role of intermediate active cellulose. *J. Anal. Appl. Pyrolysis* **2012**, *94*, 17−32.
(47) Vinu, R.; Broadbelt, L. J. A mechanistic model of fast pyrolysis of glucose-based carbohydrates to predict bio-oil composition. *Energy Environ. Sci.* **2012**, *5* (12), 9808−9826.
(48) Seshadri, V.; Westmoreland, P. R. Concerted Reactions and Mechanism of Glucose Pyrolysis and Implications for Cellulose Kinetics. *J. Phys. Chem. A* **2012**, *116*, 11997−12013.
(49) Mayes, H. B.; Broadbelt, L. J. Unraveling the reactions that unravel cellulose. *J. Phys. Chem. A* **2012**, *116* (26), 7098−7106.
(50) Zhou, X.; Nolte, M. W.; Mayes, H. B.; Shanks, B. H.; Broadbelt, L. J. Experimental and mechanistic modeling of fast pyrolysis of neat glucose-based carbohydrates. 1. Experiments and development of a detailed mechanistic model. *Ind. Eng. Chem. Res.* **2014**, *53* (34), 13274−13289.
(51) Seshadri, V.; Westmoreland, P. R. Roles of hydroxyls in the noncatalytic and catalyzed formation of levoglucosan from glucose. *Catal. Today* **2016**, *269*, 110−121.
(52) Paulsen, A. D.; Mettler, M. S.; Dauenhauer, P. J. The role of sample dimension and temperature in cellulose pyrolysis. *Energy Fuels* **2013**, *27* (4), 2126−2134.
(53) Shen, D.; Jin, W.; Hu, J.; Xiao, R.; Luo, K. An overview on fast pyrolysis of the main constituents in lignocellulosic biomass to valued-added chemicals: Structures, pathways and interactions. *Renewable Sustainable Energy Rev.* **2015**, *51*, 761−774.
(54) Antal, M. J.; Varhegyi, G.; Jakab, E. Cellulose pyrolysis kinetics: revisited. *Ind. Eng. Chem. Res.* **1998**, *37* (4), 1267−1275.
(55) Milosavljevic, I.; Suuberg, E. M. Cellulose thermal decomposition kinetics: global mass loss kinetics. *Ind. Eng. Chem. Res.* **1995**, *34* (4), 1081−1091.
(56) Teixeira, A. R.; Gantt, R.; Joseph, K. E.; Maduskar, S.; Paulsen, A. D.; Krumm, C.; Zhu, C.; Dauenhauer, P. J. Spontaneous Aerosol Ejection: Origin of Inorganic Particles in Biomass Pyrolysis. *ChemSusChem* **2016**, *9* (11), 1322−1328.
(57) Zhou, X.; Mayes, H. B.; Broadbelt, L. J.; Nolte, M. W.; Shanks, B. H. Fast pyrolysis of glucose-based carbohydrates with added NaCl part 1: Experiments and development of a mechanistic model. *AIChE J.* **2016**, *62* (3), 766−777.
(58) Branca, C.; Di Blasi, C.; Mango, C.; Hrablay, I. Products and kinetics of glucomannan pyrolysis. *Ind. Eng. Chem. Res.* **2013**, *52* (14), 5030−5039.
(59) Prins, M. J.; Ptasinski, K. J.; Janssen, F. J. Torrefaction of wood: Part 1. Weight loss kinetics. *J. Anal. Appl. Pyrolysis* **2006**, *77* (1), 28−34.
(60) Anca-Couce, A.; Obernberger, I. Application of a detailed biomass pyrolysis kinetic scheme to hardwood and softwood torrefaction. *Fuel* **2016**, *167*, 158−167.
(61) Kong, W.; Ren, J.; Wang, S.; Li, M.; Sun, R. A promising strategy for preparation of cationic xylan by environment-friendly semi-dry oven process. *Fibers Polym.* **2014**, *15* (5), 943−949.
(62) Li, S.; Chen, S.; Mu, J. Influence of UF resin on pyrolysis characteristics of biomass components: A thermogravimetric study. *Biobase Material Science and Engineering (BMSE), 2012 International Conference on*; IEEE, 2012.
(63) Moriana, R.; Zhang, Y.; Mischnick, P.; Li, J.; Ek, M. Thermal degradation behavior and kinetic analysis of spruce glucomannan and its methylated derivatives. *Carbohydr. Polym.* **2014**, *106*, 60−70.
(64) Shen, D. K.; Gu, S.; Bridgwater, A. V. Bridgwater. Study on the pyrolytic behaviour of xylan-based hemicellulose using TG−FTIR and Py−GC−FTIR. *J. Anal. Appl. Pyrolysis* **2010**, *87* (2), 199−206.
(65) Tanodekaew, S.; Channasanon, S.; Uppanan, P. Xylan/polyvinyl alcohol blend and its performance as hydrogel. *J. Appl. Polym. Sci.* **2006**, *100* (3), 1914−1918.
(66) Williams, P. T.; Besler, S. The influence of temperature and heating rate on the slow pyrolysis of biomass. *Renewable Energy* **1996**, *7* (3), 233−250.
(67) Yang, H.; Yan, R.; Chin, T.; Liang, D. T.; Chen, H.; Zheng, C. Thermogravimetric analysis− Fourier transform infrared analysis of palm oil waste pyrolysis. *Energy Fuels* **2004**, *18* (6), 1814−1821.
(68) Yu, H.; Huang, Y.; Ying, H.; Xiao, C. Preparation and characterization of a quaternary ammonium derivative of konjac glucomannan. *Carbohydr. Polym.* **2007**, *69* (1), 29−40.
(69) Zhang, X. Q.; Chen, M. J.; Liu, C. F.; Sun, R. C. Dual-component system dimethyl sulfoxide/licl as a solvent and catalyst for homogeneous ring-opening grafted polymerization of ε-caprolactone onto xylan. *J. Agric. Food Chem.* **2014**, *62* (3), 682−690.
(70) Zhou, H.; Long, Y.; Meng, A.; Li, Q.; Zhang, Y. The pyrolysis simulation of five biomass species by hemi-cellulose, cellulose and lignin based on thermogravimetric curves. *Thermochim. Acta* **2013**, *566*, 36−43.
(71) Lin, F.; Waters, C. L.; Mallinson, R. G.; Lobban, L. L.; Bartley, L. E. Relationships between Biomass Composition and Liquid Products Formed via Pyrolysis. *Front. Energy Res.* **2015**, *3*, 45.
(72) Klein, M. T.; Virk, P. S. Modeling of lignin thermolysis. *Energy Fuels* **2008**, *22* (4), 2175−2182.
(73) Yanez, A. J.; Li, W.; Mabon, R.; Broadbelt, L. J. A stochastic method to generate libraries of structural representations of lignin. *Energy Fuels* **2016**, *30* (7), 5835−5845.
(74) Zhou, S.; Pecha, B.; van Kuppevelt, M.; McDonald, A. G.; Garcia-Perez, M. Slow and fast pyrolysis of Douglas-fir lignin: Importance of liquid-intermediate formation on the distribution of products. *Biomass Bioenergy* **2014**, *66*, 398−409.
(75) Jakab, E.; Faix, O.; Till, F. Thermal decomposition of milled wood lignins studied by thermogravimetry/mass spectrometry. *J. Anal. Appl. Pyrolysis* **1997**, *40*, 171−186.
(76) Jakab, E.; Faix, O.; Till, F.; Székely, T. Thermogravimetry/mass spectrometry study of six lignins within the scope of an international round robin test. *J. Anal. Appl. Pyrolysis* **1995**, *35* (2), 167−179.
(77) Moore, A.; Park, S.; Segura, C.; Carrier, M. Fast pyrolysis of lignin-coated radiata pine. *J. Anal. Appl. Pyrolysis* **2015**, *115*, 203−213.
(78) Luo, C.; Grigsby, W.; Edmonds, N.; Easteal, A.; Al-Hakkak, J. Synthesis, characterization, and thermal behaviors of tannin stearates prepared from quebracho and pine bark extracts. *J. Appl. Polym. Sci.* **2010**, *117* (1), 352−360.
(79) Saad, H.; Khoukh, A.; Ayed, N.; Charrier, B.; Charrier-El Bouhtoury, F. Characterization of Tunisian Aleppo pine tannins for a potential use in wood adhesive formulation. *Ind. Crops Prod.* **2014**, *61*, 517−525.
(80) Mahmoud, B. S.; Saad, H.; Charrier, B.; Pizzi, A.; Rode, K.; Ayed, N.; Charrier-El Bouhtoury, F. Characterization of sumac (Rhus tripartitum) root barks tannin for a potential use in wood adhesives formulation. *Wood Sci. Technol.* **2015**, *49* (1), 205−221.
(81) Gaugler, M.; Grigsby, W. J. Thermal degradation of condensed tannins from radiata pine bark J. *J. Wood Chem. Technol.* **2009**, *29* (4), 305−321.
(82) Arbenz, A.; Avérous, L. Oxyalkylation of gambier tannin - Synthesis and characterization of ensuing biobased polyols Ind. *Ind. Crops Prod.* **2015**, *67*, 295−304.
(83) Moldoveanu, S. C. *Pyrolysis of organic molecules: Applications to health and environmental issues*; Elsevier: Amsterdam, 2009. Vol *28*.
(84) Meier, H. F.; Wiggers, V. R.; Zonta, G. R.; Scharf, D. R.; Simionatto; Ender, L. A kinetic model for thermal cracking of waste cooking oil based on chemical lumps. *Fuel* **2015**, *144*, 50−59.
(85) Stark, A. K.; Bates, R. B.; Zhao, Z.; Ghoniem, A. F. Prediction and validation of major gas and tar species from a reactor network model of air-blown fluidized bed biomass gasification. *Energy Fuels* **2015**, *29* (4), 2437−2452.
(86) Pasangulapati, V. Devolatilization characteristics of cellulose, hemicellulose, lignin and the selected biomass during thermochemical gasification: experiment and modeling studies. Ph.D. Thesis, Oklahoma State University, Stillwater, OK, 2012.

DOI: 10.1021/acssuschemeng.6b03096
ACS Sustainable Chem. Eng. 2017, 5, 2867−2881

(87) Le Brech, Y.; Ghislain, T.; Leclerc, S.; Bouroukba, M.; Delmotte, L.; Brosse, N.; Snape, C.; Chaimbault, P.; Dufour, A. Effect of Potassium on the Mechanisms of Biomass Pyrolysis Studied using Complementary Analytical Techniques. *ChemSusChem* **2016**, *9* (8), 863−872.
(88) Yildiz, G.; Pronk, M.; Djokic, M.; van Geem, K. M.; Ronsse, F.; Van Duren, R.; Prins, W. Validation of a new set-up for continuous catalytic fast pyrolysis of biomass coupled with vapour phase upgrading. *J. Anal. Appl. Pyrolysis* **2013**, *103*, 343−351.
(89) Trendewicz, A.; Evans, R.; Dutta, A.; Sykes, R.; Carpenter, D.; Braun, R. Evaluating the effect of potassium on cellulose pyrolysis reaction kinetics. *Biomass Bioenergy* **2015**, *74*, 15−25.
(90) Stefanidis, S. D.; Heracleous, E.; Patiaka, D. T.; Kalogiannis, K. G.; Michailof, C. M.; Lappas, A. A. Optimization of bio-oil yields by demineralization of low quality biomass. *Biomass Bioenergy* **2015**, *83*, 105−115.
(91) Banks, S. W.; Nowakowski, D. J.; Bridgwater, A. V. Impact of potassium and phosphorus in biomass on the properties of fast pyrolysis bio-oil. *Energy Fuels* **2016**, *30* (10), 8009−8018.
(92) Patwardhan, P. R.; Satrio, J. A.; Brown, R. C.; Shanks, B. H. Influence of inorganic salts on the primary pyrolysis products of cellulose. *Bioresour. Technol.* **2010**, *101* (12), 4646−4655.
(93) Zhu, C.; Maduskar, S.; Paulsen, A. D.; Dauenhauer, P. J. Alkaline-Earth-Metal-Catalyzed Thin-Film Pyrolysis of Cellulose. *ChemCatChem* **2016**, *8*, 818.
(94) Oasmaa, A.; Sundqvist, T.; Kuoppala, E.; Garcia-Perez, M.; Solantausta, Y.; Lindfors, C.; Paasikallio, V. Controlling the phase stability of biomass fast pyrolysis bio-oils. *Energy Fuels* **2015**, *29* (7), 4373−4381.
(95) Gargiulo, V.; Giudicianni, P.; Alfè, M.; Ragucci, R. Influence of possible interactions between biomass organic components and alkali metal ions on steam assisted pyrolysis: A case study on Arundo-donax. *J. Anal. Appl. Pyrolysis* **2015**, *112*, 244−252.
(96) Zhang, J. Fast pyrolysis behavior of different celluloses and lignocellulosic biopolymer interaction during fast pyrolysis. Master's Thesis, Iowa State University, Ames, IA, 2012.

DOI: 10.1021/acssuschemeng.6b03096
ACS Sustainable Chem. Eng. 2017, 5, 2867−2881